Electronic Supplementary Information

Plasmon-Powered Chemistry with Visible-Light Active Copper Nanoparticles

*Shreya Tyagi, Radha Krishna Kashyap, Ankit Dhankhar, and Pramod P. Pillai**

Department of Chemistry and Centre for Energy Sciences, Indian Institute of Science Education and Research (IISER), Dr. Homi Bhabha Road, Pashan, Pune – 411008, India.

Email: *pramod.pillai@iiserpune.ac.in

Section 1: Experimental details and methods

Materials and Reagents:

Copper(II) acetylacetonate ($Cu(acac)_2$) was purchased from TCI Chemicals Pvt. Ltd. India. Oleylamine, tetramethylammonium hydroxide (TMAOH) 25 % wt. in water, 11-mercaptoundecanoic acid (MUA), ammonium metavanadate (NH_4VO_3) were purchased from Sigma-Aldrich. All the reagents were used as received without any further purification. The positively charged N,N,N-trimethyl(11-mercaptoundecyl) ammonium chloride (TMA) was synthesized according to the reported procedure.[1]

Synthesis of OAm-CuNPs

Copper nanoparticles (CuNPs) were synthesized following a modified literature procedure.[2] Here, $Cu(acac)_2$ was used as the copper precursor and oleylamine was used as both a reducing agent and ligand. In a 100 mL three-neck RB flask, 66.4 mg of $Cu(acac)_2$ and 20 mL of oleylamine were mixed and heated to 100 °C with continuous stirring. The reaction was degassed for 30 min. After this, it was continuously purged with argon followed by heating the reaction mixture upto 230 °C for 2 h to obtain a clear red colloidal solution. The solution was purified by precipitating the solution with (1:15) ratio of toluene and methanol, followed by centrifugation. Finally, the purified OAm-CuNPs were redispersed in toluene and used for further studies. The synthesis of CuNPs is

challenging as it is susceptible to undergo oxidation. Adequate precautions were taken to prevent the oxidation, such as (i) maintaining the inert atmosphere throughout the synthesis, (ii) purification with degassed solvents, (iii) minimal exposure of CuNPs during purification, and (iv) redispersion in a degassed solvent. These precautions turned out to be decisive in maintaining the long-term stability of the CuNPs in our study.

Synthesis of [+] and [-] CuNPs

[+] and [-] CuNPs were prepared using a ligand exchange of OAm-CuNPs with (*N,N,N* trimethyl(11-mercaptoundecyl)ammonium chloride (TMA, [+]) and 11-mercaptoundecanoic acid (MUA, [-])), respectively. In a typical synthesis of [-] CuNPs, 10 mM solution of MUA ligand in 10 mL dichloromethane was added to the purified OAm-CuNPs dispersed in toluene, which triggered the aggregation and precipitation of CuNPs. The solution was left undisturbed for 2 h for complete ligand exchange. Next, the supernatant was decanted, and the precipitate was washed with dichloromethane (2 x 10 mL) and acetone (10 mL) to remove all the excess OAm and MUA ligands. The precipitate was then dried and redispersed in Milli-Q water by adding 20 µL of tetramethyl ammonium hydroxide (25 wt. % in water) to deprotonate the carboxylic acid group in MUA. A similar procedure was adopted for the synthesis of [+] CuNPs with TMA as the incoming ligand. Both [+] and [-] CuNPs showed a sharp LSPR band at ~580 nm in water.

Synthesis of OAm-AuNPs

Oleylamine-capped gold nanoparticles (AuNPs) were synthesized following a modified literature procedure.[3] In a 100 mL three-neck RB flask, 5 mL of oleylamine was taken and then the solution was refluxed at 150 °C under an inert atmosphere. This was followed by a rapid injection of a solution containing 0.3 mmol of $HAuCl_4.3H_2O$ and 1 mL of oleylamine. The reaction mixture was heated for 1.5 h for the complete growth of the AuNPs. After that, the reaction mixture was allowed to cool down to room temperature and 1 mL of toluene was added to quench the reaction. The solution was purified by adding ethanol into the nanoparticle solution in a 2:1 (v/v) ratio, followed by centrifugation at 5000 rpm for 5 minutes. Finally, the purified OAm-AuNPs were redispersed into toluene and used for further studies.

Section 2: Instrumentation and techniques used

UV-visible absorption studies: UV-vis absorbance data were recorded on a Shimadzu UV-3600 spectrophotometer in a quartz cuvette of 1 cm path length.

Transmission electron microscopy (TEM): The TEM samples were prepared by drop casting the copper nanoparticle solution on a 400-mesh carbon-coated copper grid (Tedpella Inc.), followed by drying under vacuum. The High-Resolution Transmission Electron Microscopic (HRTEM) imaging was performed on the JEOL JEM2200FS (200 kV) HRTEM instrument.

Powder X-ray diffraction (PXRD) measurements: Powder X-ray diffraction patterns were measured at room temperature on Bruker D8 Advanced X-Ray Diffractometer using Cu K_α (λ = 1.54 Å) rays and processed using PDXL software.

SERS studies: Raman spectra were collected using a laser source having an excitation wavelength of 632.8 nm on a Raman microscope (LabRAM HR, HoribaJobinYvon) and with an acquisition time of 10 seconds using a 50x objective (spectral resolution of the system is ~1 cm^{-1}).

X-ray photoelectron spectroscopy (XPS) studies: The XPS study was performed by drop casting the CuNPs on a silicon wafer followed by drying under the vacuum. Then the measurements were performed in Thermo Fisher Scientific Instrument, Leicestershire, UK (Model: K-Alpha+) equipment using Al-Kα anode (1486.6 eV) in a transmission lens mode and multi-channel plate (MCP) detector. The binding energy scale was calibrated using standard C 1s peak (284.6 eV) and the elemental peaks were analysed using non-linear Shirley background correction. The peak positions fitting was performed by using XPSPEAK41 software and optimized by a weight least-square fitting method using Gaussian and Lorentzian lineshape.

Dynamic light scattering (DLS) and Zeta (ζ) potential measurements: The dynamic light scattering and zeta potential measurements of charged CuNPs were measured in Zetasizer Nano series, Nano-2590 (Malvern instruments, U.K.). The optical density of the nanoparticle solution was maintained at ~0.1 during all the measurements. ζ was determined by measuring the electrophoretic mobility and using Henry's equation:[4]

$$U_E = \frac{2\varepsilon\zeta f(k_a)}{3\eta}$$

Where,

U_E is the electrophoretic mobility

ε is the dielectric constant

ζ is the zeta potential (mV)

η is the viscosity coefficient of the medium (Pa.s)

$f(k_a)$ is Henry's function determined using Smoluchowski's approximation

The error was estimated from three different measurements on three different samples.

Inductively coupled plasma-mass spectrometry (ICP-MS): ICP-MS measurement was performed with Quadrupole-ICP MS (Thermo iCAP-Q) instrument to determine the concentration of the CuNPs. The copper standards were prepared to have 5, 10, 15, and 20 ppb concentrations in 0.32 N HNO_3 solution. The CuNP samples were prepared in 0.32 N HNO_3 solution by digesting with a minimal amount of aqua regia.

Section 3: Synthesis of CuNPs

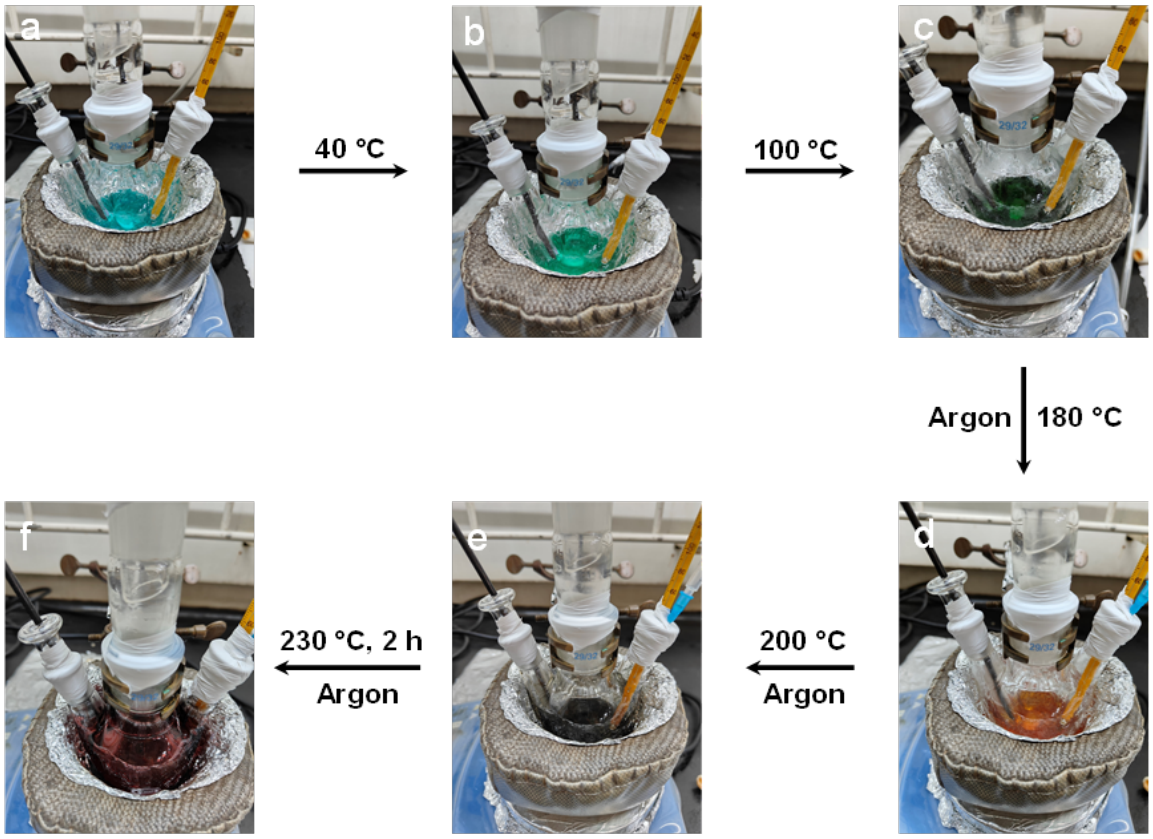

Fig. S1 Experimental setup for the synthesis of oleylamine-capped copper nanoparticles (OAm-CuNPs).[2] Optical photographs showing the colour change of the solution during the synthesis over time.

Section 4: Characterization of CuNPs

Transmission electron microscopy (TEM) analysis:

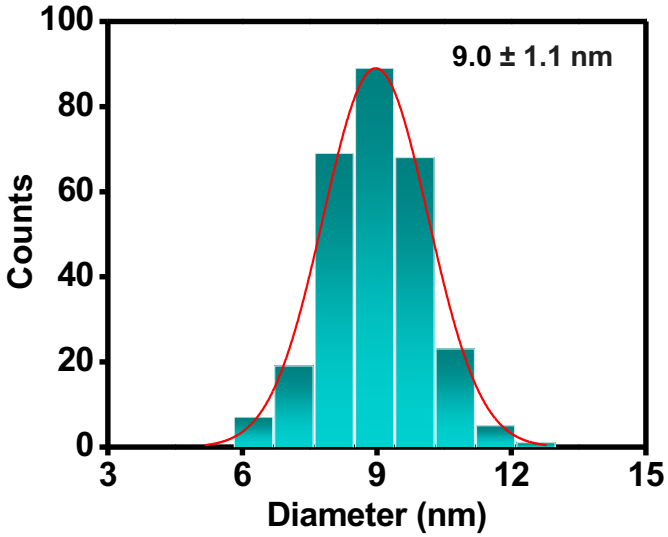

Fig. S2 A histogram showing the size distribution of OAm-CuNPs. An average diameter was calculated to be 9.0 ± 1.1 nm (from ~300 NPs).

Determination of molar extinction coefficient of CuNPs:

The molar extinction coefficient of CuNPs was estimated using ICP-MS, TEM and UV-vis studies.

Size of the particle, d (calculated from TEM) = 9.0 ± 1.1 nm

Volume of one nanoparticle = $\frac{4}{3}\pi r^3 = \frac{4}{3}\pi(\frac{d}{2})^3$ = 381.51 nm^3

Lattice constant of Cu = 0.362 nm

Volume of unit cell, a^3 = 0.0474 nm^3

Copper crystallizes in face centered cubic unit cell with a lattice constant (a) of 0.362 nm with 4 atoms in a unit cell.

Total number of copper atoms in one nanoparticle, A is given by below equation:

$$N = \frac{4}{3}\pi(\frac{d}{2})^3 * (\frac{4}{V_{unit\ cell}})$$

N = 32195

Therefore, no. of copper atoms in one nanoparticle, N =32195.

The number of moles of copper in the given solution calculated from ICP-MS data is 0.020 x 10^{-9} moles.

The molar extinction coefficient (ε) was determined using the Beer-Lambert law.

$$A = \varepsilon\, c\, l$$

Where,

A = Absorbance or optical density

ε = Molar extinction coefficient (M^{-1} cm^{-1})

c = Concentration of the solution (mol L^{-1})

l = Optical path length = 1 cm

A= 0.516

C = no. of moles per unit volume (in L)

= 0.020 x 10^{-9} / (0.003 L) = 6.66 x 10^{-9} mol L^{-1}

$\varepsilon = \frac{A}{c}$ = 0.516/(6.66 x 10^{-9}) M^{-1} cm^{-1}

= 7.7 x 10^{7} M^{-1} cm^{-1}

The molar extinction coefficient (ε) is found to be **7.7 x 10^{7} M^{-1} cm^{-1}**.

X-ray photoelectron spectroscopy (XPS) measurements:

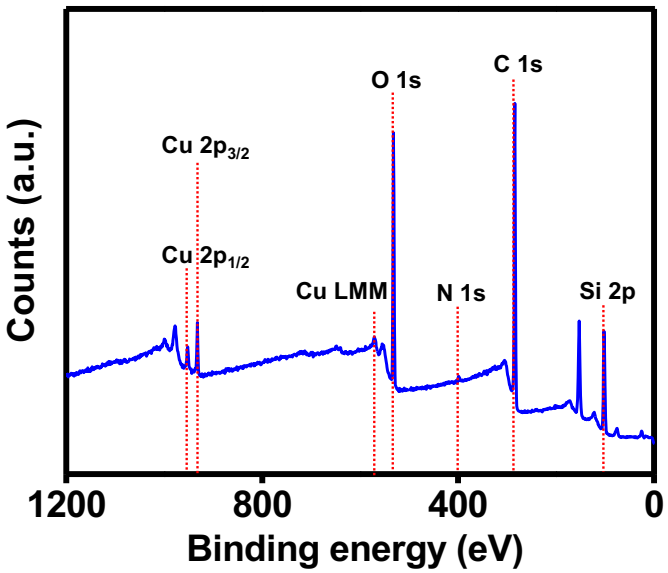

Fig. S3 XPS survey spectrum of OAm-CuNPs confirms the presence of all major elements in CuNPs. The peak at 101.9 eV corresponds to Silicon 2p as the sample was drop cast on a silicon wafer.

Section 5: Stability studies

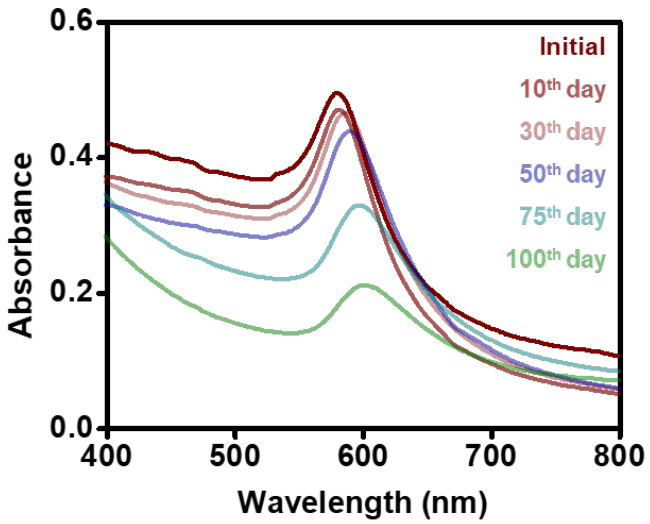

Fig. S4 Time-dependent UV-vis absorption spectra of OAm-CuNPs redispersed in toluene. A sharp LSPR peak was observed at ~580 nm. The OAm-CuNPs were stable in toluene for at least for 50 days, with a marginal shift in the LSPR band by ~8 nm. After 50 days, prominent bathochromic and hypochromic shift was observed.

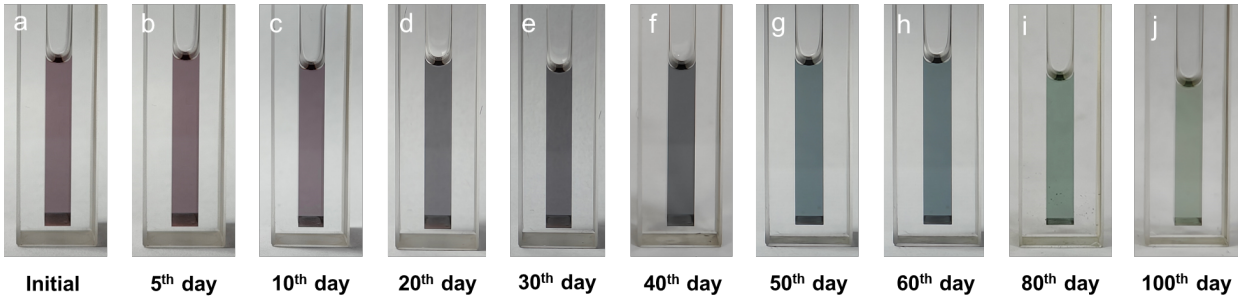

Fig. S5 Optical photographs of OAm-CuNPs redispersed in toluene. The OAm-CuNPs were stable in toluene for at least 50 days. A color change from wine-red to bluish-red to greenish color was observed, corresponding to ~20 nm shift in the LSPR band after 100 days.

Under inert conditions

In a typical experiment, ~50 µL of [-] CuNP from a ~0.4 µM stock solution were taken in a 3 mL long-neck cuvette containing 3 mL degassed Milli-Q water (conc: ~6.5 nM in terms of NP and O.D.= 0.5). The cuvette was sealed with a septum followed by Argon purging for 15 minutes. The colloidal stability of [-] CuNPs was then monitored through time-dependent UV-vis absorption studies. A negligible change in the UV-vis absorption characteristics was observed for at least ~ 2 days ($\Delta\lambda_{LSPR}$ ~4 nm), confirming the stability and retention of the plasmonic color (see inset of Fig. 3 and Fig. S6). Similarly, keeping all the experimental parameters unchanged, the stability study was performed for [+] CuNP. Here again, a marginal change in the UV-vis absorption features ($\Delta\lambda_{LSPR}$ ~2 nm) was observed for ~2 days, confirming the colloidal and compositional stability of [+] CuNPs (Fig. S7).

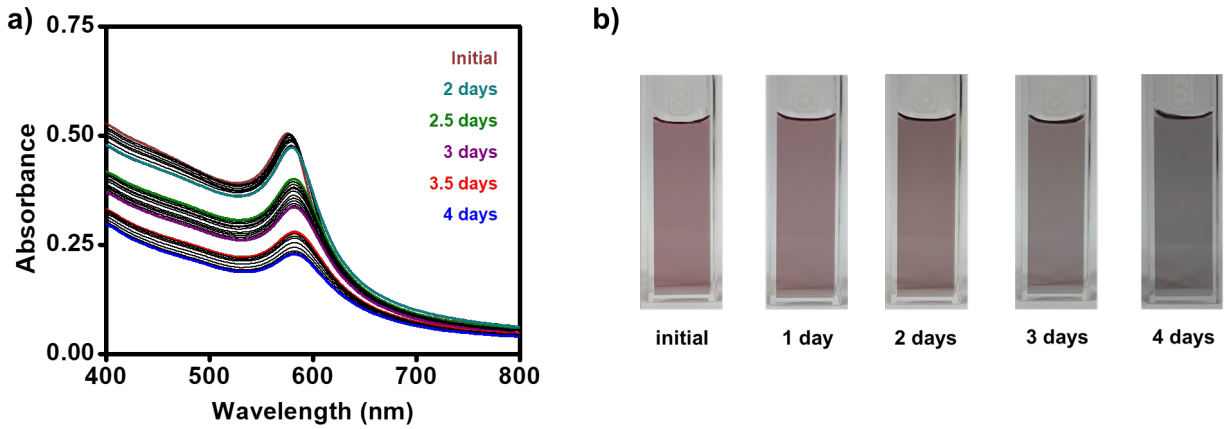

Fig. S6 Stability study of [-] CuNP. (a) Time-dependent UV-vis spectra of [-] CuNPs redispersed in water. A sharp LSPR peak was observed at ~576 nm. A negligible change in the UV-vis absorption was observed for at least ~ 2 days ($\Delta\lambda_{LSPR}$ ~4 nm), confirming the stability and retention of the plasmonic color. After that a gradual red-shift in LSPR peak was observed, along with the broadening of the peak as well as a decrease in the absorbance. This indicates the oxidation of [-] CuNPs. (b) Optical photographs of [-] CuNPs at different time intervals. A color change from wine-red to blackish was observed after ~ 4 days, corresponding to ~6 nm shift in the LSPR band.

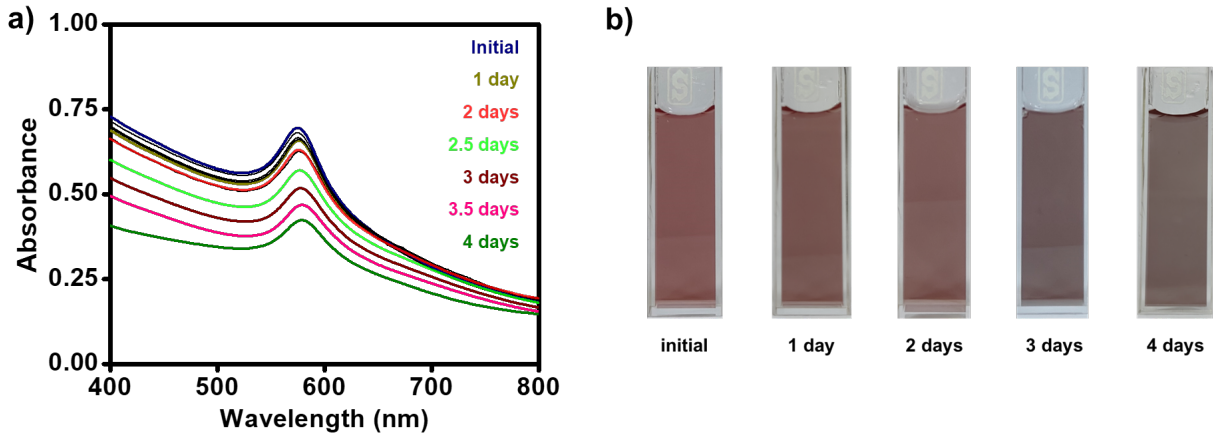

Fig. S7 Stability study of [+] CuNP. (a) Time-dependent UV-vis spectra of [+] CuNPs redispersed in water. A sharp LSPR peak was observed at ~575 nm. A negligible change in the UV-vis absorption was observed for at least ~ 2 days ($\Delta\lambda_{LSPR}$ ~2 nm), confirming the stability and retention of the plasmonic color. After that a gradual red-shift in LSPR peak was observed, along with the broadening of the peak as well as a decrease in the absorbance. This indicates the oxidation of [+] CuNPs. (b) Optical photographs of [+] CuNPs at different time intervals. A color change from wine-red to brownish-black was observed after ~ 4 days, corresponding to ~4 nm shift in the LSPR band.

Under ambient conditions

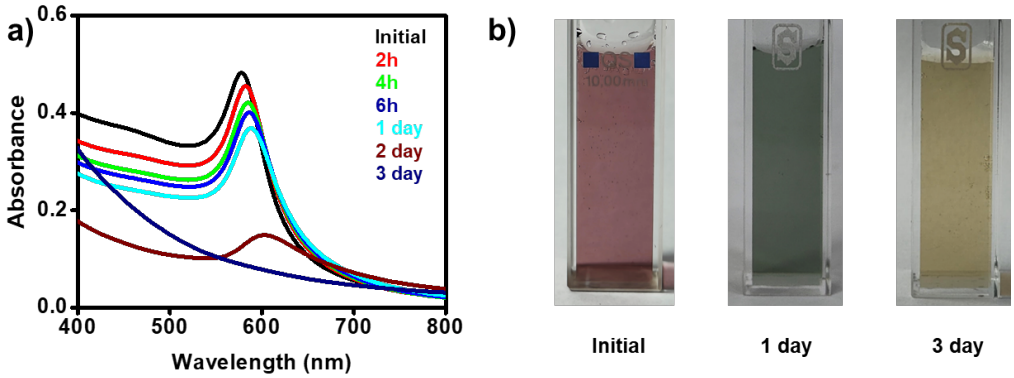

Fig. S8 Stability study of [-] CuNP. (a) Time-dependent UV-vis spectra of [-] CuNPs redispersed in water. A sharp LSPR peak was observed at ~580 nm. The [-] CuNPs are stable in water for 6 h and over this period LSPR peak was red-shifted along with the broadening of the peak and decrease in absorbance, as CuNPs gradually got oxidized. (b) Optical photographs showing the color change during the stability study.

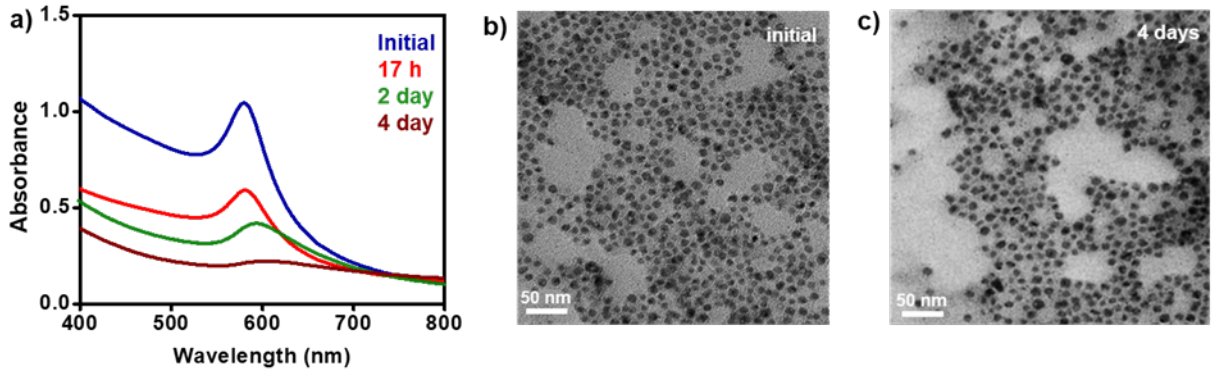

Fig. S9 Stability study of [+] CuNP. (a) Time-dependent UV-vis absorption spectra of [+] Cu NPs redispersed in water. A sharp LSPR peak was observed at ~580 nm. The [+] CuNPs were stable in water for one day and over this period SPR peak was red-shifted along with the broadening of the peak and decrease in absorbance, as CuNPs gradually got oxidized. Representative TEM images of the corresponding CuNPs taken (b) immediately after the synthesis and (c) after 4 days.

Section 6: Photothermal conversion efficiency, photostability and thermal stability

Photothermal conversion efficiency of CuNPs (under 532 nm illumination)

In a typical experiment, 10 µL of CuNP (~9 nM in terms of NPs) was drop cast over the glass slide which was kept inside the glass cuvette having 1 mL water. The film was irradiated using ~1 W 532 nm continuous wave diode laser. The simultaneous rise in temperature was measured using a thermocouple dipped in the solution (the thermocouple was attached to a digital multimeter Model 17B$^+$ ESP; Fluke, Everrit, Washington, USA). A control experiment was carried out with only water (without CuNP) keeping all the other parameters constant (**Fig. S10, Movie S1**†).

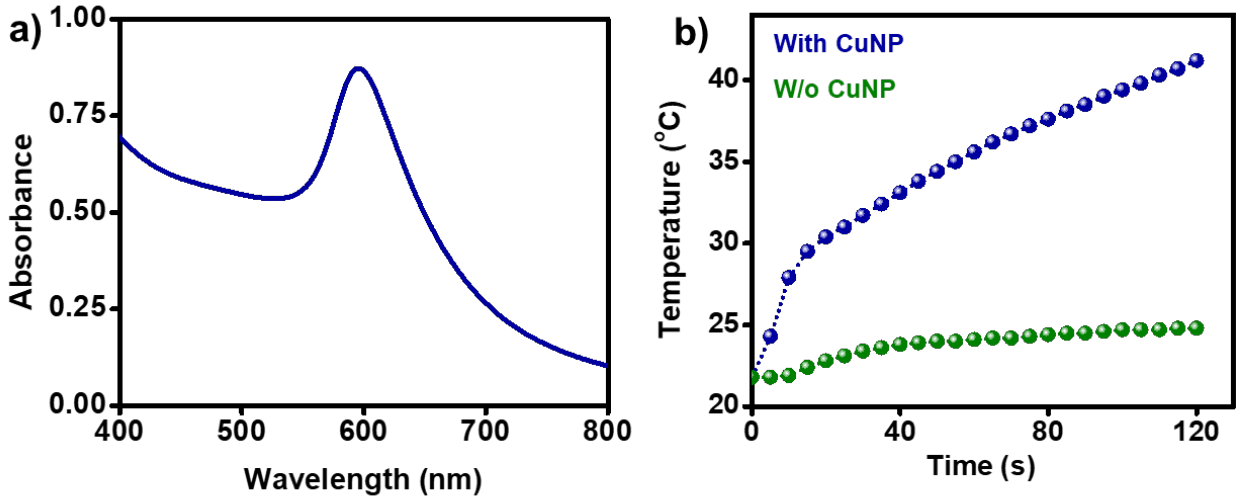

Fig. S10 Photothermal conversion efficiency measurement. (a) UV-vis absorption spectrum of the OAm-CuNP dispersed in toluene. (b) Measurement of temperature rise in 1 mL water with (blue) and without (green) CuNPs, under constant irradiation using a 532 nm CW diode laser. The light intensity at the cuvette wall was measured to be 1 W.cm^{-2}.

Following a modified Roper's method,[5] the photothermal conversion efficiency (η_{PT}), was calculated using the equation:

$$\eta_{PT} = \frac{hS\,(T_{max} - T_{surr}) - Q_{dis}}{I(1 - 10^{-A_{532}})} \qquad (1)$$

Where,

η_{PT} = Photothermal conversion efficiency

h = Heat transfer coefficient

S = Surface area of the container

T_{max}= Maximum temperature achieved with CuNPs under irradiation (41.2 ℃, see **Fig. S10b**)

T_{surr}= Temperature before irradiation (21.8 ℃, see **Fig. S10b**)

Q_{dis} = Heat dissipated by light illumination without CuNPs

I = Light intensity (1 W)

A_{532} = Absorbance at 532 nm (0.53 OD, see **Fig. S10a)**

hS can be expressed as

$$hS = \frac{m_s C_s}{\tau_s} \qquad (2)$$

where,

m_s= mass of the water (1000 mg)

C_s= specific heat capacity of the water (4.2 J g^{-1} $℃^{-1}$)

τ_s= time of the irradiation (120 s)

Therefore,

$$hS = \frac{1000 \times 4.2}{120}\ mW\ ℃^{-1}$$

$$= \mathbf{35\ mW\ ℃^{-1}}$$

Q_{dis} can be calculated from the control experiment with only water in the absence of CuNPs

$$Q_{dis} = \frac{mC\Delta T}{t} \qquad (3)$$

Where,

m = mass of water (1000 mg)

C= specific heat capacity of water (4.2 J g^{-1} $℃^{-1}$)

ΔT = temperature increase in water (3 ℃, see **Fig. S10b**)

t = time of the irradiation (120 s)

Therefore,

$$Q_{dis} = \frac{1000 \times 4.2 \times 3}{120}\ mW$$

$$= \mathbf{105}\ \boldsymbol{mW}$$

By substituting all the values in equation (1), the photothermal conversion efficiency (η_{PT}) was calculated to be **81.4%**

Photostability studies

The photostability studies have been carried out in solution state for an illumination time of 2 h. The colloidal solution of OAm-CuNP in toluene was taken in a 3 mL cuvette (~7.8 nM in terms of NPs) and illuminated with 1 W 532 nm CW diode laser for 2 h (light intensity falling on the cuvette wall was estimated to be 1W.cm^{-2}). The stability was monitored through time-dependent UV-vis absorption studies. The data was collected initially in time intervals of 10 minutes and later in intervals of 30 minutes, as shown in Fig. S11a,b. A negligible change in the absorption features with time confirms the excellent photostability of OAm-CuNP under prolonged laser illumination. Likewise, both the solution and solid-state (CuNP film) were found to be stable for ~10 min under focused solar irradiation (Fig. S11c,d).

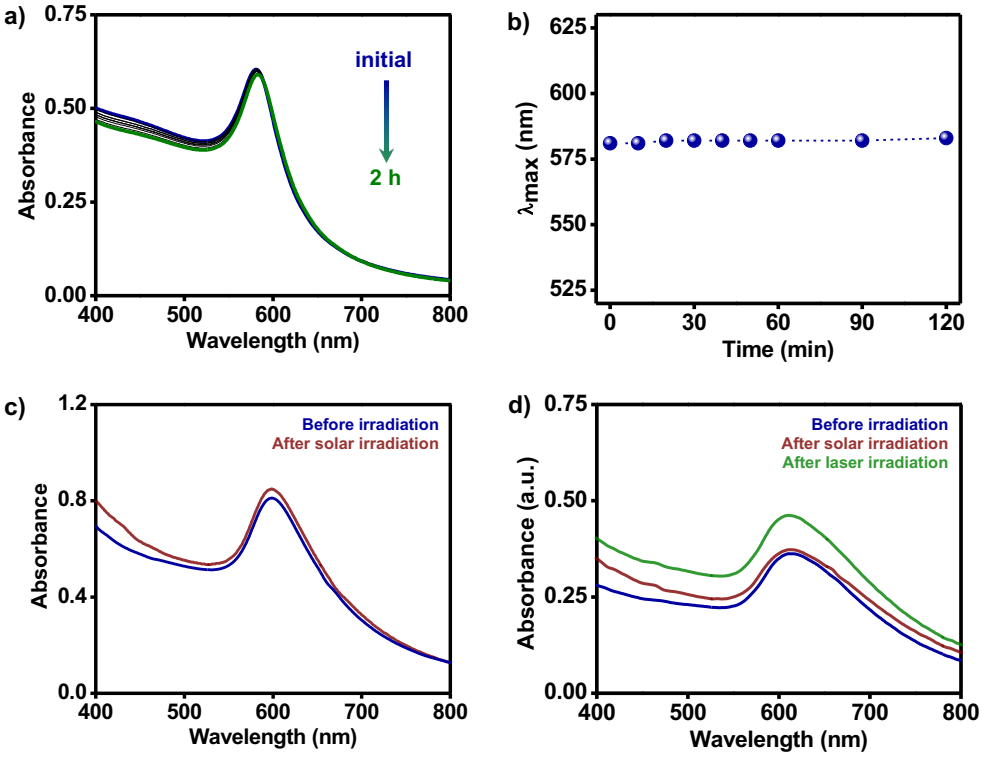

Fig. S11 Photostability study of OAm-CuNP in solution and solid states. (a) UV-vis absorption spectra of OAm-CuNPs dispersed in toluene monitored at different time intervals of continuous irradiation with a 532 nm CW diode laser for 2 h (the intensity falling on the cuvette wall was estimated to be 1 W.cm^{-2}). (b) Negligible change in λ_{LSPR} was observed over a time of 2 h of continuous laser irradiation, confirming the prolonged photostability of OAm-CuNP in colloidal state. (c) UV-vis absorption spectra of OAm-CuNPs dispersed in toluene before and after 10 min of solar illumination. (d) Solid-state UV-vis absorption spectra before and after 10 min light irradiation as mentioned in the figure legends. The solid-state absorption was measured under the reflectance mode. Diffuse reflectance data was converted to absorbance using the Kubelka-Munk transformation.

Thermal stability of CuNPs

The thermal stability of OAm-CuNPs was studied in two temperature ranges: 25-100 °C (in toluene) and 25-200 °C (in the reaction medium, oleylamine).

25-100 °C (in toluene): The thermal stability of OAm-CuNPs dispersed in toluene was studied in the temperature range of 25-100 °C, under ambient conditions using a temperature controller (SHIMADZU Temperature Controller TCC-100). In a typical experiment, a 3 mL toluene solution of OAm-CuNP (~ 12 nM in terms of NPs) was prepared in a glass vial and then kept in a temperature controller for 2 minutes at a particular temperature (with a step size of 10 °C). Next, the corresponding UV-vis absorption was measured (Fig. S12a). A negligible change in the UV-vis absorption characteristics and plasmonic color was observed, which confirms the stability of OAm-CuNPs in toluene till 100 °C (Fig S12b).

25-200 °C (in the reaction medium, oleylamine): To test the thermal stability at higher temperatures (up to 200 °C), the experiment was performed in oleylamine under inert atmosphere. In a typical experiment, the as-synthesized OAm-CuNPs (without purifying) were allowed to cool down to room temperature followed by a gradual increase in the temperature from 25 °C to 200 °C (with a step size of 25 °C). Different aliquots were taken out after 2 min at each temperature, followed by UV-vis absorption measurements. A negligible change in the UV-vis absorption characteristics and plasmonic colour was observed, which confirms the stability of OAm-CuNPs till 200 °C (Fig S13). As unpurified OAm-CuNPs were used, an increase in scattering was seen at ~800 nm with time.

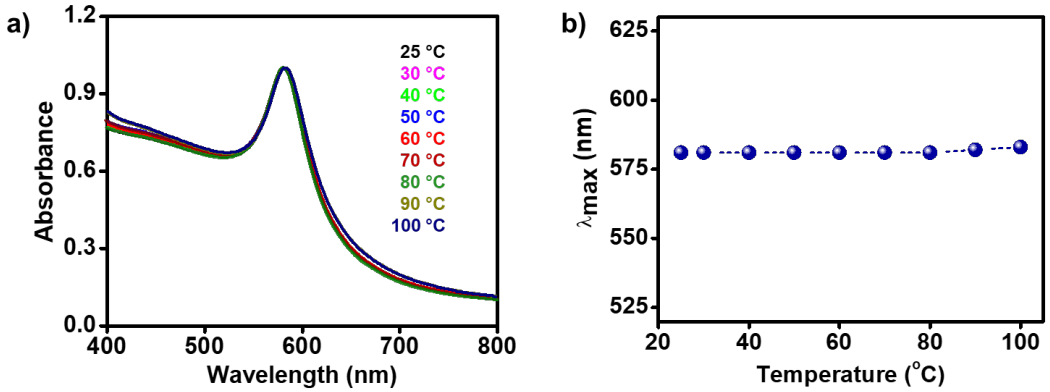

Fig. S12 Thermal stability study of OAm-CuNP in toluene. (a) UV-vis absorption spectra of OAm-CuNPs heated at different temperatures. (b) A negligible change was observed in the λ_{LSPR} upon heating at various temperatures, which confirms the thermal stability of OAm-CuNPs till 100 °C in toluene.

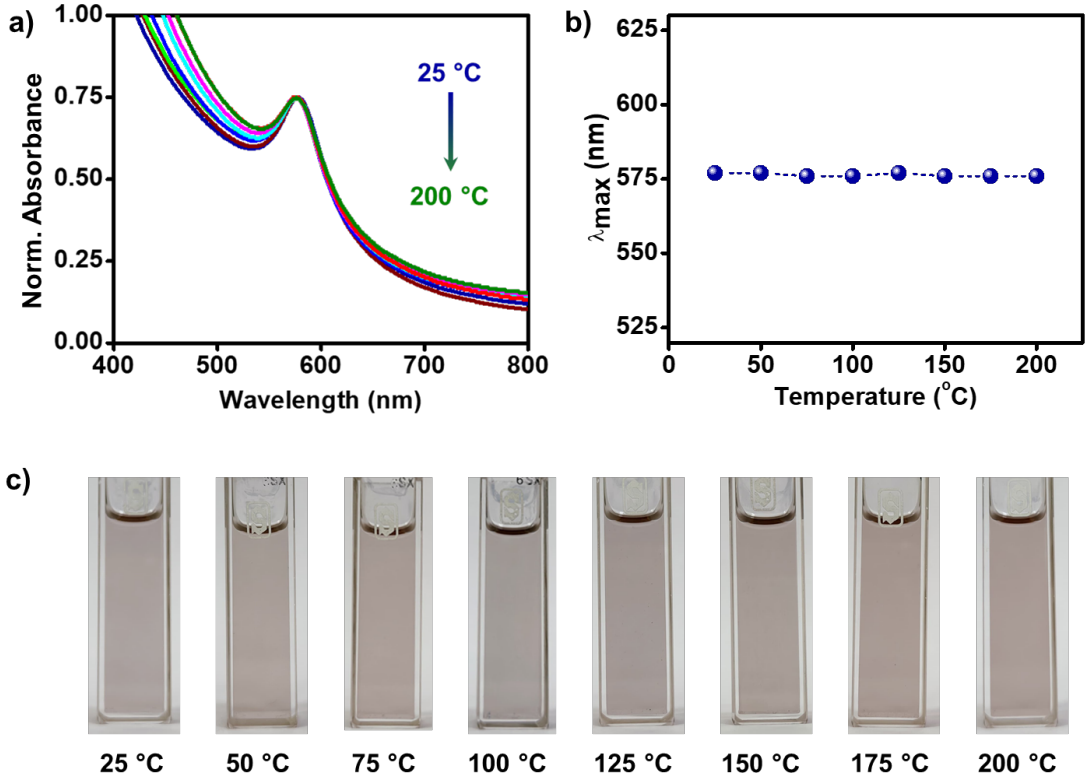

Fig. S13 Thermal stability study of as-synthesized OAm-CuNP in oleylamine. (a) UV-vis absorption spectra of the OAm-CuNP heated at different temperatures. (b) A negligible change was observed in the λ_{LSPR} upon heating at various temperatures, which confirms the thermal stability of OAm-CuNPs till 200 °C in oleylamine. As unpurified OAm-CuNPs were used, an increase in scattering was seen at ~800 nm with time. (c) Optical photographs of colloidal OAm-CuNPs at different temperatures.

Synthesis and characterisation of OAm-AuNPs

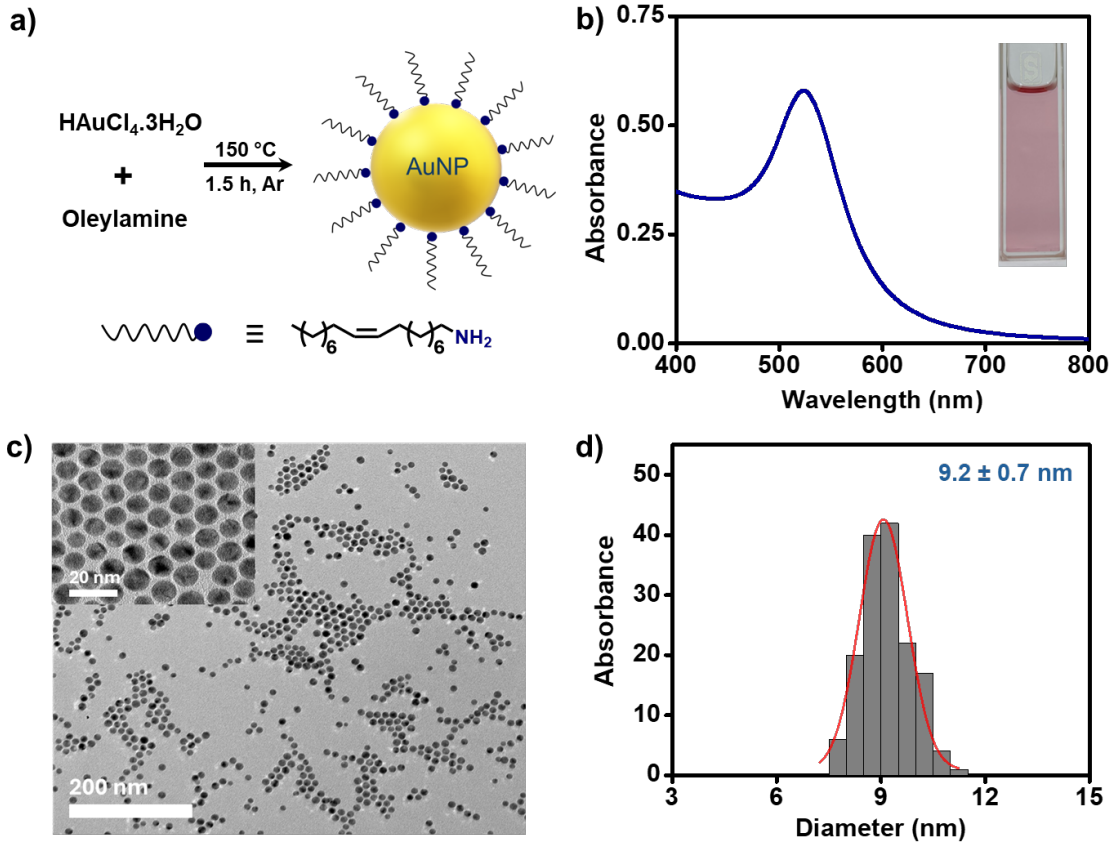

Fig. S14 Synthesis and characterization of OAm-AuNPs. (a) Schematic representation of the synthesis of OAm-AuNPs. (b) UV-vis absorption spectrum of OAm-AuNPs in toluene showing the characteristic LSPR band at ~524 nm, along with its optical photograph in the inset. (c) A representative TEM image of OAm-AuNPs. (d) A histogram showing the size distribution of OAm-AuNPs. The average diameter was calculated to be 9.2 ± 0.7 nm (from ~150 NPs).

Photothermal conversion efficiency of AuNPs (under 532 nm illumination)

In a typical experiment, a film of OAm-AuNPs was made on a glass slide by drop casting 12 µL of 0.75 µM OAm-AuNPs (~9 nM in terms of NPs). The area of OAm-AuNPs film was ~ 0.8 cm^2, which is similar to the one made for OAm-CuNPs. The concentration of AuNPs was kept similar to that of CuNPs. Next, the OAm-AuNPs coated glass slide was immersed in a glass cuvette containing 1 mL MilliQ water and irradiated with a 1 W 532 nm continuous wave diode laser (light intensity falling on the cuvette wall was estimated to be 1 $W.cm^{-2}$). The simultaneous rise in temperature was measured using a thermocouple dipped in the solution (the thermocouple was attached to a digital multimeter Model $17B^+$ ESP; Fluke, Everrit, Washington, USA). A control

experiment was carried out with only water (without AuNP) keeping all the other parameters constant (Fig. S15).

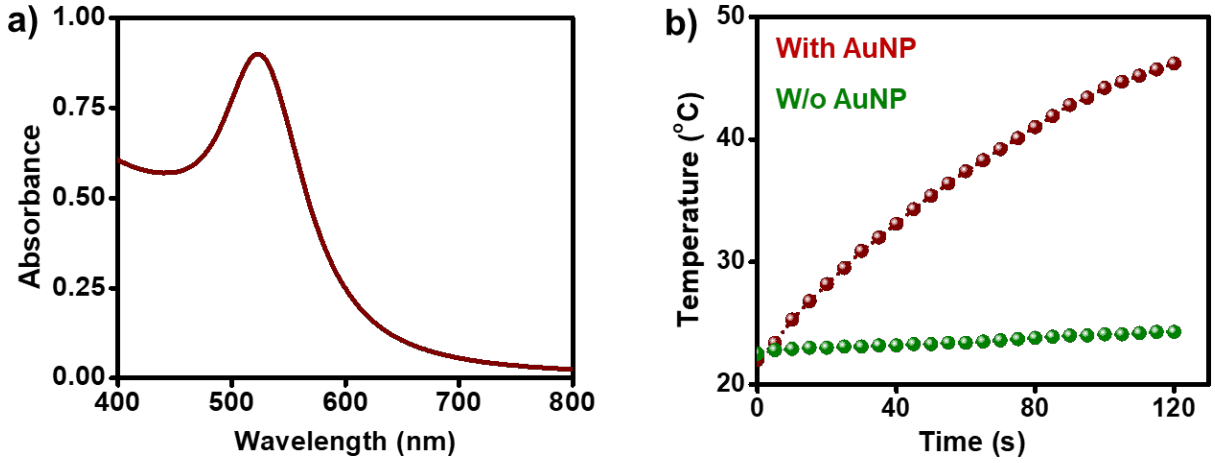

Fig. S15 Photothermal conversion efficiency measurement. (a) UV-vis absorption spectrum of ~9 nM OAm-AuNP (in terms of NPs) dispersed in toluene. (b) Measurement of temperature rise in 1 mL water with (wine) and without (green) OAm-AuNPs coated glass slide, under constant irradiation with a 532 nm CW diode laser. The light intensity at the cuvette wall was measured to be 1 W.cm^{-2}.

By substituting all the values in equation (1), the photothermal conversion efficiency (η_{PT}) was calculated to be **90.6%**

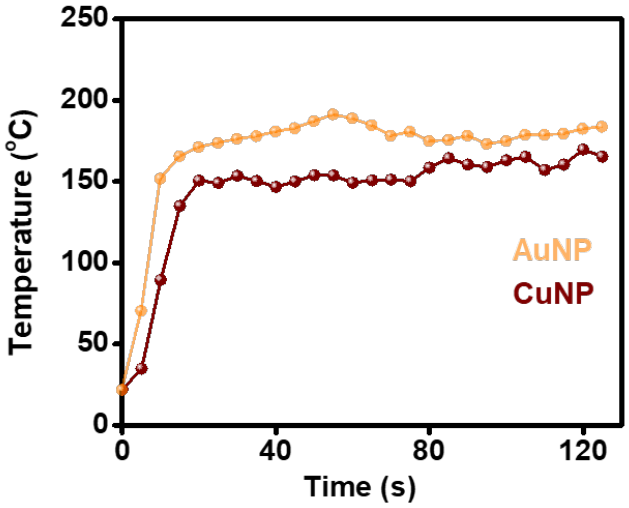

Fig. S16 A plot showing the temperature rise measured in the presence of 9.0 ± 1.1 nm OAm-CuNP and 9.2 ± 0.7 nm OAm-AuNP, under irradiation with an 1W 532 nm CW diode laser . A sharp temperature rise was observed immediately after the laser illumination of the NP films, which got saturated at ~170 °C (ΔT~150 °C) and ~190 °C (ΔT~170 °C) within 30 s of illumination of CuNP and AuNP films, respectively. The light intensity at the cuvette wall was measured to be 1 W.cm^{-2}. It must be noted that the concentration

of both OAm-AuNP and OAm-CuNP was same (~9 nM in terms of NPs). Area of OAm-AuNP and OAM-CuNP films was ~ 0.8 cm^2 on a ~3 cm^2 Al foil.

Section 7: Solar-vapor generation studies

In a typical experiment, 8 mL of DI water was taken in a 30 mL test tube containing the CuNP film on a glass slide. Sunlight was focused onto the CuNPs immersed in water using a Fresnel lens (19.5 cm x 28.5 cm). A control experiment was performed without CuNP while keeping all other parameters the same. The Movie S2† clearly shows the solar-vapor generation and condensation of water on the sides of the test tube in the presence of CuNP. Vigorous boiling along with big bubbles was observed after 2 min. Whereas, in the case of the control experiment, no such boiling was observed.

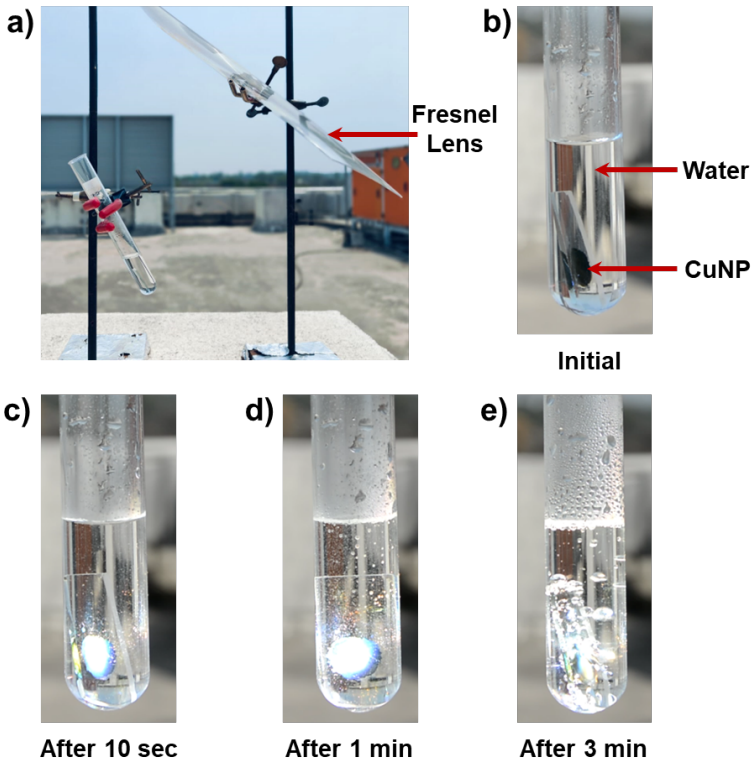

Fig. S17 (a) Photograph of the experimental setup for solar-vapor generation. Photograph of a test tube containing a CuNP film on a glass slide immersed in 8 mL of DI water (b) before, (c) after 10 sec, (d) after 1 min, and (e) after 3 min of solar irradiation.

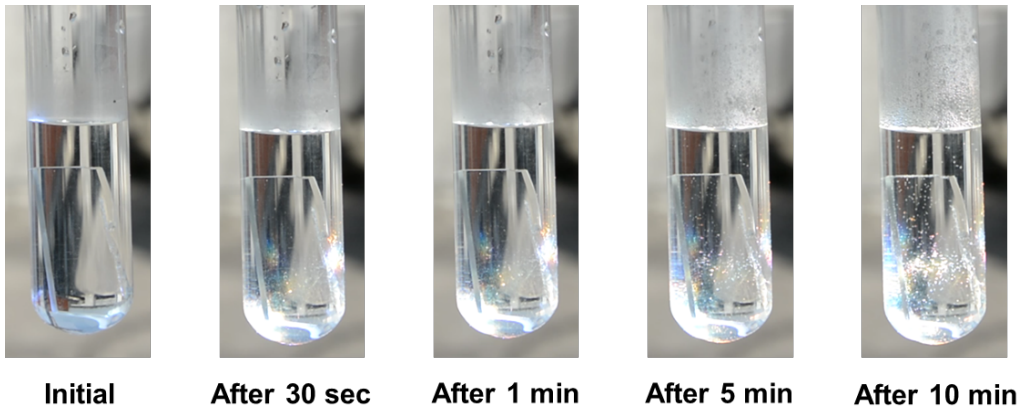

Fig. S18 Photographs of test tubes containing 8 mL water in the absence of CuNP at different time intervals of focused solar irradiation.

Quantification of solar-vapor generation:

In a typical experiment, ~6 mL of DI water and OAm-CuNP film on a glass slide were taken in a 3.5 cm wide Petri dish. The Petri dish was then placed onto a weighing balance (Mettler Toledo ME403/04) with 1 mg readability to monitor the weight loss. A thermocouple was attached to note down the temperature variations. Sunlight was focused on the CuNP film immersed in water, the spot diameter was fixed to be 1 cm using a Fresnel lens having a dimension of 14 cm x 20 cm. The solar power measured was 8.0 $W.cm^{-2}$ using an optical power sensor (Model LM-10 HTD; Coherent, Santa Clara, CA 95054 USA), under our experimental conditions. ~3 mg loss of water was observed within 24 min of irradiation, whereas ~1 mg was lost in the case of the control experiment without CuNP.

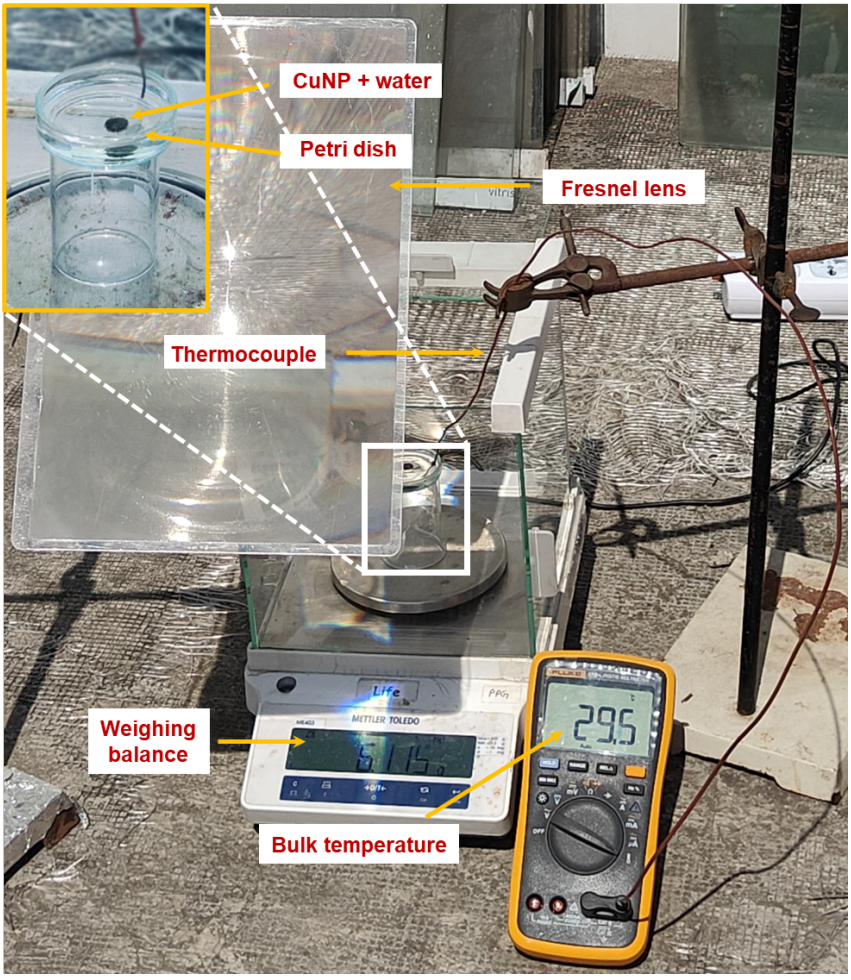

Fig. S19 Experimental setup for monitoring the weight loss and temperature rise during the plasmonic heat-driven solar-vapor generation with OAm-CuNPs.

Calculation of evaporation rate:

The evaporation rate was calculated using the equation:[6]

$$\text{Evaporation rate} = \frac{\Delta m}{A\Delta T}$$

Where, Δm (in kg) is the mass loss of water during the time interval ΔT (in h), and A (in m^2) is the area.

The evaporation rate was ~7.7 kg m^{-2} h^{-1} when the area of the Petri dish (d=3.5 cm) was taken into account in the calculation.

Calculation of solar-vapor generation efficiency:

The thermodynamic equivalent reaction flow chart for the process of solar vapour generation, under our experimental condition is shown in **Equation S1.**

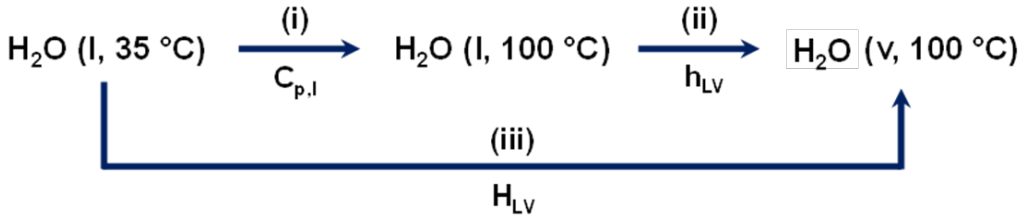

Equation S1. Thermodynamic equivalent reaction flow chart for solar vapour generation under our experimental condition.

According to Hess's law,[5] the overall enthalpy of water evaporation, H_{LV}, is equal to the sum of the enthalpies for processes (i) and (ii)

$$\eta_{SVG}(\%) = \frac{Q_{LV}}{Q_{input}} \times 100 = \frac{mH_{LV}}{q_i C_{opt}} \times 100$$

Where,

η_{SVG} = efficiency of solar-vapor generation,

Q_{LV} = energy consumed during water evaporation,

Q_{input} = energy of the incident solar radiation,

m = mass loss of water after evaporation (~3 g),

H_{LV} = enthalpy of liquid to vapor phase transformation, which includes specific heat capacity of water, Cp (4.18 J K^{-1} g^{-1}) as well as latent heat of vaporization, $h_{LV,373K}$ (2257.2 J g^{-1}), i.e., H_{LV} = ($C_P\Delta T + h_{LV}$)

q_i = power of illuminated solar light (8.0 W.cm^{-2}),

C_{opt} = optical concentration, which is obtained by multiplying the power with spot area (1 cm^2).

$$\eta_{SVG}(\%) = 3\ g \times \frac{[\{4.18\ JK^{-1}g^{-1} \times (373\ K - 308\ K)\} + 2257.2\ Jg^{-1}]}{8.0\ Wcm^{-2} \times 1\ cm^2 \times 1440\ s} \times 100$$

$$\eta_{SVG}(\%) = \sim \mathbf{66}\%$$

Table S1: Comparison table with conventional solar light absorbers

S. No.	Materials	Light Source	Final Temp (°C)	Evaporation rate (kg m^{-2} h^{-1})	Efficiency (%)	References
1	AuNPs	Focused Sunlight	80	2.5 g in 4 min	24	*ACS Nano,* 2013, **7** , 42–49
2	Bundled AuNR array	Focused sunlight	80	20.5	93	*Chem. Mater.,* 2022, **34** , 7369–7378
3	Black Au	Solar simulator (1-20 kW m^{-2})	80	1-16	25-57	*Nat. Commun.*, 2015, **6** , 10103–10111
4	AgNPs and poly (sodium-p-styrenesulfonate , PSS) on agarose gel	Solar simulator (1 kW m^{-2})	-	2.1	92.8	*Adv. Funct. Mater.*, 2019, **29**, 1901312
5	CuNP-cauliflower (micro-nanostructure)	Solar simulator (1 kW m^{-2})	49	-	62	*Nanoscale*, 2016, **8** , 14617
6	CuNPs clusters on cellulose membrane	Solar simulator (2 kW m^{-2})	60 in 3 h	-	73	2019 *Nanotechnology*, 2019, **30 ,** 015402
7	**CuNPs**	**Focused sunlight**	**75**	**7.7**	**66**	**This work**

As can be seen from Table S1, the efficiency and temperature rise caused by OAm-CuNPs are better or comparable to the previously reported CuNPs (please compare entries 5 and 6 with entry 7). Au and Ag based plasmonic NPs in entries 2 and 4 have better parameters compared to our CuNPs. It must be noted that entry 2 in Table S1 is for anisotropic Au nanostructures (bundled gold nanorods), which is having 2-3 orders of higher molar absorption cross-section than spherical AuNPs. Likewise, entry 4 in Table S1 is for AgNP deposited on an agarose-based hydrogel, which is expected to enhance the water contact with AgNPs. Hence, entries 2 and 4 are expected to show better photothermal properties compared to spherical hydrophobic nanoparticles. Importantly, the spherical CuNPs synthesized in this work show comparable properties with spherical AuNPs (please compare entries 1 and 7). The added advantage of CuNPs is the cost-effectiveness, which

makes them an affordable alternative to conventional plasmonic NPs for various visible-light-driven processes. In future, the photothermal properties of CuNPs can be further improved by using a support system, as well as by installing anisotropy to Cu nanostructures (like rod, cube, etc.). In summary, the solar vapour generation properties of plasmonic CuNPs reported in the present work are one of the best among the Cu-based nanostructures reported so far and comparable with the benchmark spherical AuNPs.

Section 8: Thermochromic studies

Ammonium metavanadate (NH_4VO_3) was used as thermochromic material in our study.[7] In a typical experiment, around 5 mg ammonium metavanadate was placed on CuNPs, and irradiated with a 1 W 532 nm continuous wave laser for ~20 min under ambient conditions. The color changes were captured using the Macro Zoom Fluorescence Microscope System (Olympus MVX10) at 5X magnification. The photographs were taken at different time intervals. A control experiment was carried out without CuNPs i.e., only glass substrate, under the same condition.

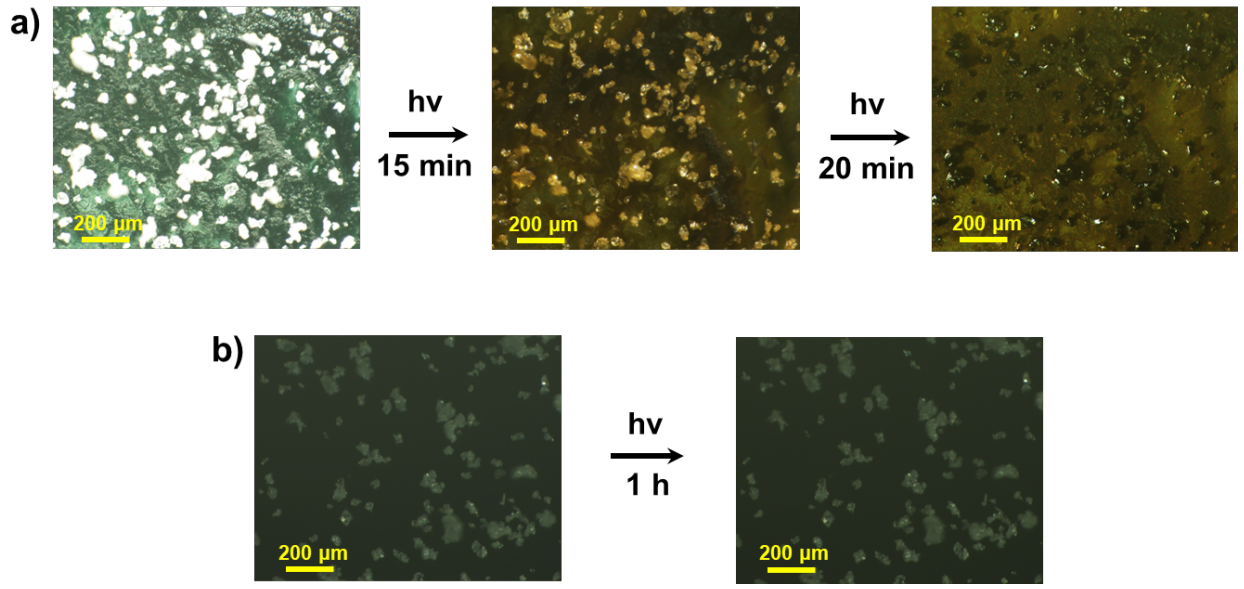

Fig. S20 (a) Optical microscopic image showing the magnified area of CuNP film (green area) over which there is a uniform distribution of ammonium metavanadate (white powder). A colour change from white to yellow followed by black was observed after irradiation with 1W 532 nm continuous wave laser (light intensity was estimated to be 1 $W.cm^{-2}$) for ~20 min. (b) Photographs obtained before and after irradiation of ammonium metavanadate on a glass slide (without CuNP film) for ~1 h. No colour change was observed.

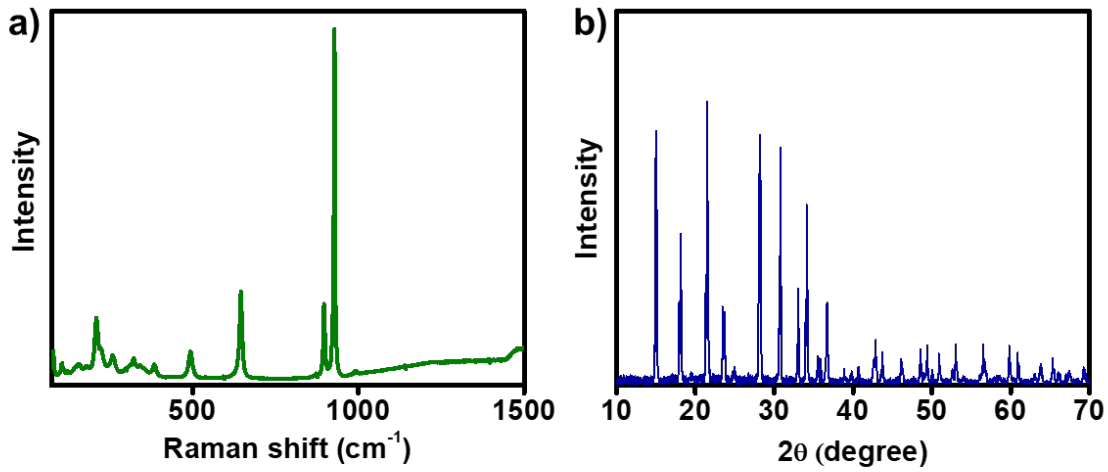

Fig. S21 (a) Raman analysis and (b) PXRD patterns of NH_4VO_3 placed on a glass slide (without CuNP coating) after irradiation with 1W 532 nm continuous wave laser (light intensity was estimated to be 1 $W.cm^{-2}$).

References

1. J. Tien, A. Terfort and G. M. Whitesides , *Langmuir*, 1997, **13** , 5349-5355.
2. Y. Wang, Q. Zhang, Y. Wang, L. V. Besteiro, Y. Liu, H. Tan, Z. M. Wang, A. O. Govorov , J. Z. Zhang, J. K. Cooper, J. Zhao, G. Chen, M. Chaker and D. Ma , *Chem. Mater.*, 2021, **33** , 695-705.
3. S. Liu , G. Chen , P. N. Prasad and M. T. Swihart , *Chem. Mater.*, 2011, **23** , 4098-4101.
4. D. C. Henry , *Proc. R. Soc. Lond.*, 1931, **A133** , 106-129.
5. D. K. Roper, W. Ahn and M. Hoepfner , *J. Phys. Chem. C*, 2007, **111** , 3636–3641.
6. Q. Zhu, K. Ye, W. Zhu, W. Xu, C. Zou, L. Song, E. Sharman, L. Wang, S. Jin, G. Zhang, Y. Luo and J. Jiang , *J. Phys. Chem. Lett.*, 2020, **11** , 2502– 2509.
7. A. A. Akande, E. C. Linganiso, B. P. Dhonge, K. E. Rammutla, A. Machatine, L. Prinsloo, H . Kunert and B. W. Mwakikunga , *Mater. Chem. Phys.*, 2015, **151** , 206–214.